CLASSIFICATION STRATEGIES FOR POLARIMETRIC SAR SEA ICE DATA

Bernd Scheuchl[(1)], Irena Hajnsek[(2)], Ian Cumming[(1)]

[(1)] *Department of Electrical and Computer Engineering, University of British Columbia 2356 Main Mall, Vancouver, B.C. Canada V6T 1Z4 Email: berdns@ece.ubc.ca, ianc@ece.ubc.ca*

[(2)] *German Aerospace Centre, Microwaves and Radar Institute, Department SAR Technology, P.O. Box 1116, 82234 Wessling, Germany Email: irena.hajnsek@dlr.de*

ABSTRACT / RESUME

Bayesian classification of polarimetric data is based on the complex Wishart distribution of the coherency matrix. The classifier has shown to be a flexible tool available in a variety of options. In this paper we investigate several classification strategies for sea ice classification. All methods show reasonable results, although some user input prior to classification seems beneficial. Noise and incidence angle were found to affect the classification result, the latter due to a change in the relative mix of scattering mechanisms. Surface scattering is found to be strongly incidence angle dependent. Multi-frequency data have a superior information content and can separate ice types, whereas the scattering information content can not be exactly discriminated using only C-band data.

1 INTRODUCTION

The complex Wishart classifier has been proven to be a powerful tool for the classification of polarimetric SAR data [1]. It can be applied to polarimetric data and, in a modified version, even to multi-polarization data (i.e. dual or alternating polarization). An extension to multi-frequency data is also possible. The algorithm is very robust against changes in initialisation [2] thus allowing a variety of options for the application of the method. An overview of possible classification strategies is given in Section 2. In this paper we investigate two airborne polarimetric SAR data sets of sea ice: a three-frequency AIRSAR scene and a CV-580 C-band scene. Both scenes have been processed using different options for the iterative Wishart classifier.

Spaceborne single polarization SAR data are used operationally for information extraction from ice centres around the world. ENVISAT-ASAR, RADARSAT-2 and ALOS PALSAR will provide multi-polarization and polarimetric data thus allowing further automation in the classification of ice types present. Promising results were achieved in the past using the Wishart classifier for the information extraction over sea ice [2].

2 WISHART CLASSIFICATION STRATEGIES

Possible options for the use of the Wishart method are shown in Fig. 1, including the fully supervised direct classification based on operator selected training areas. For operational use a more automated approach is desirable. Class interpretation (i.e. assignment of classes to ice types) is required for all results with one exception.

One option is to fix a set of classes (e.g. with the $H/A/\alpha$ classifier), thus avoiding user interaction during the classification process. If some knowledge of the scene is available, the number of classes can be restricted and the class interpretation effort can be reduced. But the restriction of the number of classes is an interaction and the classifier is not longer automated.

The highest degree of automation is achieved by incorporating the interpretation of scattering mechanisms in the classification procedure [3]. Since, the method was developed for land applications, it cannot be used to its full extent for sea ice applications. C- band backscatter of sea ice is largely dominated by surface scattering. While volume scattering is also present (particularly for Multi Year Ice), this restricts the utilisation of the classification method. Class interpretation will again be required in this case.

Three options for classification are applied in this paper and are outlined in Fig. 1. In all cases 12 iterations were chosen for the Wishart classifier. Two additional options were also tested which resulted in a significantly higher computational effort without improving the result.

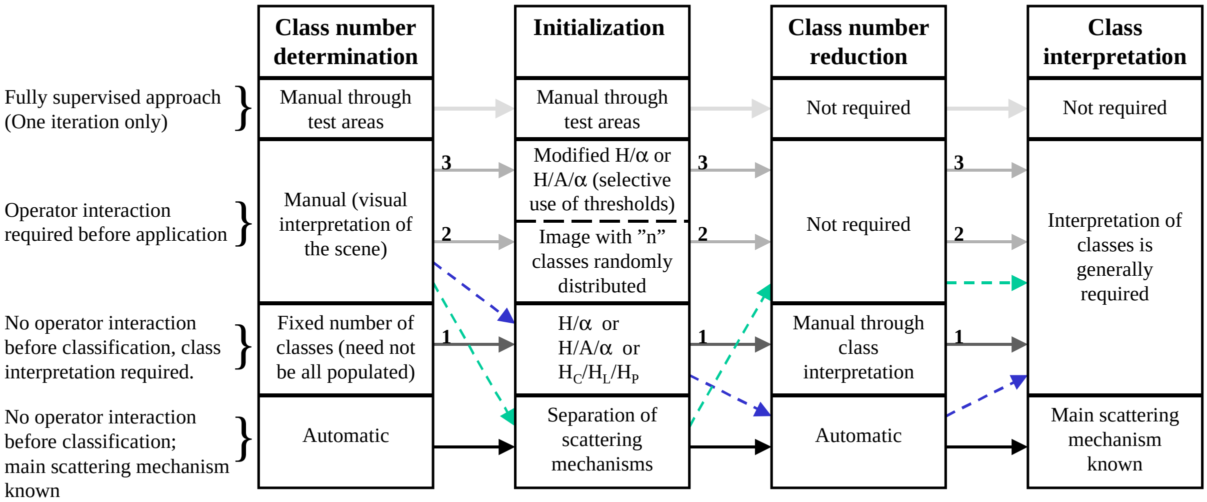

Fig. 1. Options for applying the Wishart classifier. Two possible additional methods are shown in dashed lines. The numbers indicate the options presented in this paper: 1: Fig 3(iii), 2: Fig. 3(iv), and 3: Fig.4.

3 AVAILABLE DATA AND CLASSIFICATION RESULTS

The three classification strategies shown in Fig. 1 are tested on two data sets. With no exact solution known, only one relative comparison between results is shown. In this example, three frequency data are compared to C-band data, thus illustrating the higher information content of multi-frequency data.

3.1 AIRSAR data set

In 1988 the National Aeronautics and Space Administration/Jet Propulsion Laboratory (NASA/JPL) acquired SAR data of sea ice in the Beaufort Sea using the airborne AIRSAR system. Polarimetric SAR data in C-, L-, and P-band were collected. The scene used for this study is scene 1372. It was acquired on March 11, 1988 with scene center coordinates 73.048ºN and 142.285ºW and incidence angles from 27º to 52º. The pixel spacing for the data is 6.7 m in slant range and 12.1 m in azimuth (4 look images). Additional averaging of 2x2 pixels was applied before data analysis to reduce the effect of speckle.

The test site is characterised by Multi Year Ice (MYI) with floe thickness up to 6 m (hummocks) with compressed First Year Ice (FYI) surrounding the floes. Smooth and ridged FYI cover the rest of the area [4]. The average thickness of the FYI near an ice camp, set up near the acquisition site, was reported to be 1.5 m. Fig. 2 shows the total power images for the three frequencies as well as a false colour composite of the three images with a description of the ice types present in the scene. The large floes shown in red in the RGB composite image in Fig. 2 are MYI. They show the highest return for C-band. The longer L-and P-band wavelengths penetrate deep into the sea ice volume and therefore have little return likely due to significant signal loss. Compressed FYI (CFYI) shown in white surrounds the MYI floes. The web of light blue lines indicates ridged FYI and rubble (RFYI/R). Dark blue areas are smooth FYI (SFYI) and the black features indicate leads, covered in Thin Ice (ThI). The scene interpetation is taken from [4].

A classification of the three frequency data by thresholding each of the three Entropy images is shown in Fig. 3(i). The result is not very accurate but serves well as input for an iterative Wishart classifier (see Fig. 3(ii)). All eight classes are subsequently assigned to ice types and, with only five ice types present (two of which are not separated), the number of classes has been manually reduced to four (see Fig. 3(iii)). The corresponding colour assignment is shown in Table 1 and compares well with the ice type discussion above. Leads and smooth FYI are not separated, though. The 8-class classification clearly shows an incidence angle effect in the classification result, this effect is best visible for the MYI feature (see Fig. 3(ii), white and grey).

As RADARSAT-2 will collect fully polarimetric data in C-band only, a classification with one frequency has been processed and is shown in Fig. 3(iv). The confusion matrix, comparing the C-band and the three frequency results, is given in Table 2. There are two apparent groups of ice types: ThI, SFYI, RFYI/R and CFYI, MYI. While there is little confusion between the two groups, confusion within those groups can be significant. Again, the leads can not be separated from smooth FYI. Leads are important for ice monitoring as they allow efficient navigation.

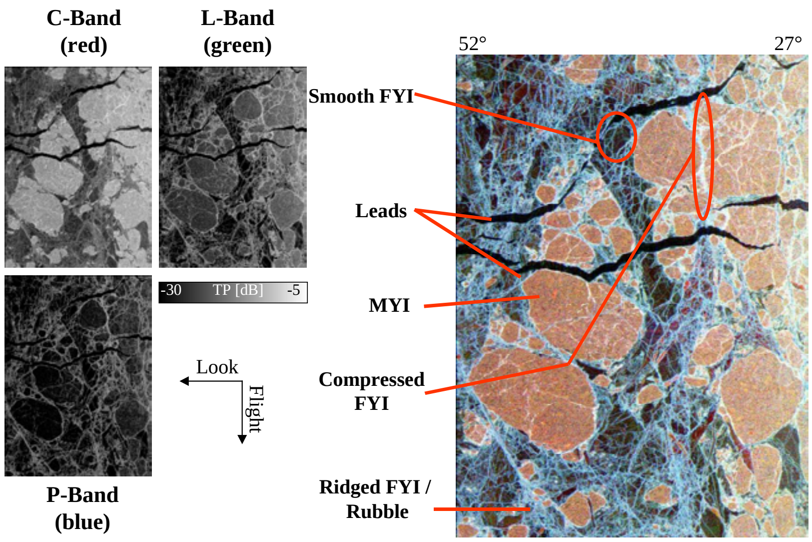

Fig. 2. AIRSAR Total Power images (left) and polarimetric RGB composite (right). Test site: Beaufort Sea. Scene center coordinates: 73.048ºN and 142.285ºW.

Table 1. Colour assignment for AIRSAR classification result (see Fig. 3).

Ice Type	Colors	Description
ThI / SFYI	blue	New forming Thin Ice / Smooth First Year Ice
RFYI / R	orange, (green), (black)	Ridged First Year Ice / Rubble
CFYI	pink, (pastell green)	Compressed First Year Ice
MYI	white, (gray)	Multi Year Ice

Table 2. Confusion matrix for C-band result vs. three frequency classification result (see Fig. 3).

		Reference: C-, L-, and P-band (iii)			
		ThI / SFYI	**RFYI / R**	**CFYI**	**MYI**
C-band (iv)	**ThI / SFYI**	97.09%	44.02%	0.01%	0.01%
	RFYI / R	2.91%	54.38%	11.24%	4.00%
	CFYI	0.00%	0.00%	38.48%	19.15%
	MYI	0.00%	1.60%	50.27%	76.84%

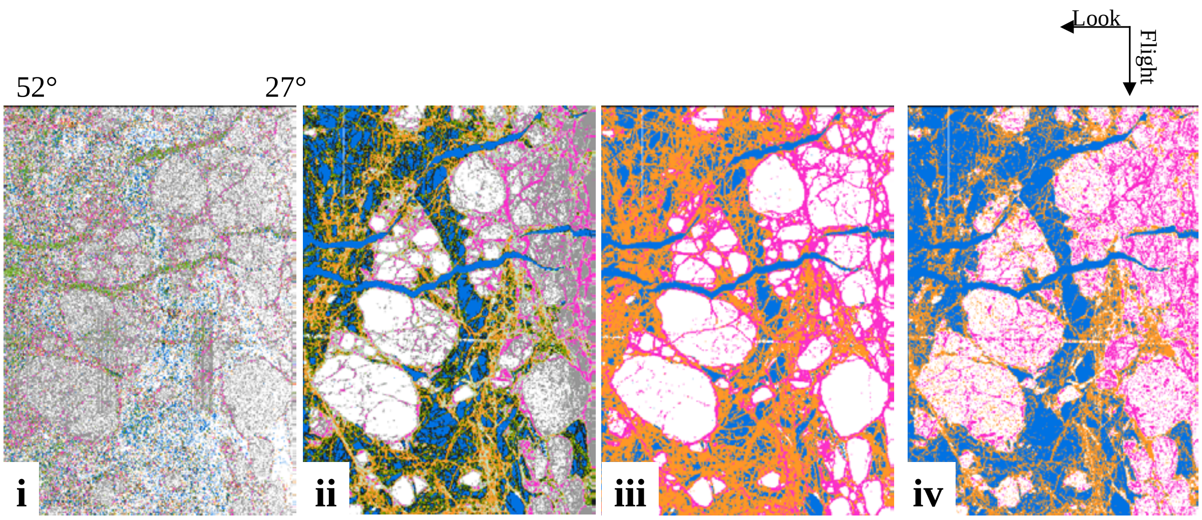

Fig. 3. Classification results using (i) Entropy thresholds of 0.5 for each frequency, (ii) Iterative Wishart classifier initialised with this result, (iii) C-, L-, P-band classification result after manual class merge, and (iv) C-band only classification result (see Table 2 for confusion matrix). Colour assignments and ice classes are given in Table 1.

3.2 CV-580 data set

On March 8, 2001, the Environment Canada CV-580 airborne SAR acquired fully polarimetric SAR data in several test areas near Prince Edward Island, Canada. An RGB colour composite using the channel information HH, HV and VV is shown in Fig. 4. The scene covers 6.4 km in slant range and approximately 8 km in azimuth and was acquired in the Northumberland Strait. SLC data with a pixel size of 4 m in (slant-) range and 0.43 m in azimuth are available. To reduce the effect of speckle noise, the data are multi-looked (40 looks in azimuth and 4 looks in range) resulting in a pixel size of approximately 17 m in azimuth and 16 m in slant range. Climate reports for the area indicate an extended melt-free period prior to data acquisition.

The polarimetric RGB composite image reveals six different ice types in the image, four of which are FYI. Leads and new forming ice are also present in the scene (see Table 4). Based on this initial assessment, the H/α classifier was slightly modified to obtain six classes. The thresholds used are given in Table 3. The class means are then used to initialise an iterative Wishart classification. Fig. 4 shows the classification result; the corresponding colour assignment is described in Table 4.

All classes show good agreement with the ice types described in Table 4. In contrast to the AIRSAR classification result, the leads are separated from ice. Two main reasons can be given for this. Firstly, the NESZ of the CV-580 system is–40 dB, about 5 dB lower than the AIRSAR NESZ. Secondly, due to the higher resolution of the CV-580 data, more pixels were averaged. No MYI is present in the scene, this may have some affect on the classifier.

Table 3. Thresholds for the modified H/α classifier to obtain 6 classes (see Fig. 4)

$H < 0.5$	$\alpha > 52.5°$		$H > 0.5$	$\alpha > 52.5°$
	$40° < \alpha < 52.5°$			$40° < \alpha < 52.5°$
	$\alpha < 40°$			$\alpha < 40°$

Table 4. Colour assignment for CV-580 classification result (see Fig. 4)

Class #	Colour	Ice Type
1	Grey	Thin, new forming ice (ThI)
2	Magenta	FYI (floes, far range)
3	White	rough FYI (strong HV)
4	Green	ridged FYI
5	Blue	Leads
6	orange	FYI (floes, near range)

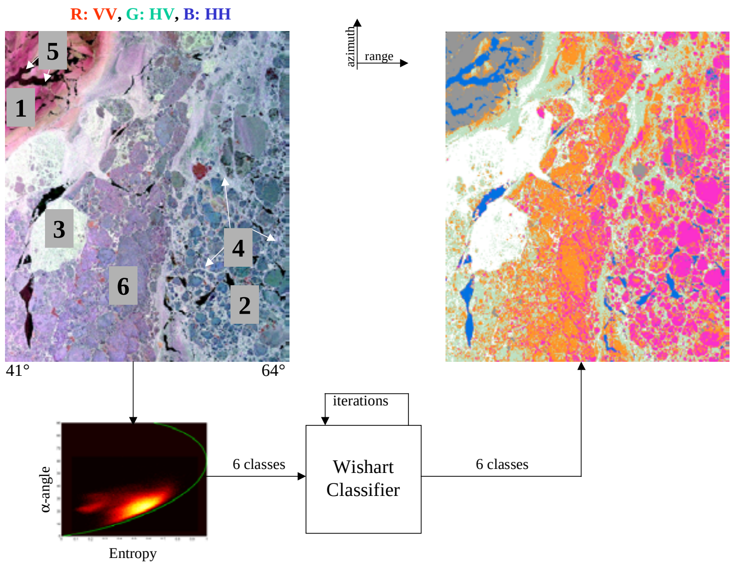

Fig. 4. CV-580 polarimetric RGB composite (left) and classification result (right). Test site: Northumberland Strait. The Wishart classifier is initialized using a modified H/α classifier (thresholds used are given in Table 3, the colour assignment is shown in Table 4).

4 INCIDENCE ANGLE DEPENDENCE OF POLARIMETRIC PARAMETERS AND IMPLICATIONS FOR WISHART CLASSIFICATION

Using the CV-580 data, a number of polarimetric parameters are tested for incidence angle dependence (see Fig. 5). The main reason for investigating the incidence angle is to understand its influence on the Wishart classification result. Based on the classification result (see Fig. 4), the parameters are averaged over azimuth for each class separately.

The α-angle is a measure for the average scattering mechanism, and is found to increase with incidence angle. α-values $< 40°$ indicate predominately surface scattering. With the increase we can deduce that the surface scattering component of the ice decreases with increasing incidence angle.

The scattering Entropy (H), the measure for the amount of different scattering mechanisms, also increases with increasing incidence angle. An observed decrease in channel correlation also shows a reduction in surface scattering, as surface scattering is the main scattering type that leads to high correlation.

The Freeman-Durden total power components [5] as well as the eigenvalues of the coherency matrix are direct estimates for the intensities of the scattering mechanisms. The first eigenvalue over sea ice can be interpreted as surface scattering [6] and indeed it shows strong similarities to the Freeman-Durden surface scattering component. The two curves differ mainly in strength. Volume scattering and double bounce scattering, as well as the smaller two eigenvalues, do not show a significant incidence angle dependence.

The classification result in Fig. 3(ii) is clearly affected by the incidence angle. As shown in this section, it is the relative mixture in scattering mechanism that changes with incidence angle, mainly due to the incidence angle dependency of the surface scattering. For the example shown in Fig. 3(ii), the number of classes used is larger than the number of ice types separable using the Wishart classifier. In this case, up to three classes are assigned to one ice type. The MYI is divided in a near range MYI class and a far range MYI class. Restricting the number of classes to four (as shown for C-band only in Fig. 3(iv)), no incidence angle effect can be observed. It is therefore important to carefully select the number of classes or take the incidence angle effect into account for class interpretation. Another option would be to compensate for incidence angle variations.

5 CONCLUSIONS

The Wishart classifier is a versatile tool for the classification of single- and multi-frequency polarimetric SAR data. From fully supervised to fully automated classification, a variety of strategies exist that vary in their requirement for user interaction.

For sea ice classification, a semi-automated method with some prior knowledge of the scene seems most effective. User interaction is possible before and after classification. In the first case, the number of ice types observed is used to set the number of classes for the classifier. The number of classes can also be fixed (e.g. by the choice of the initialisation method), in this case the resulting classes need to be merged manually to reflect the number of ice types (assuming more classes than ice types).

The strength of scattering decreases with increasing incidence angle, thus affecting the classification result. This needs to be taken into account in class interpretation. Restriction of the number of classes to the number of ice types present in the scene has shown to reduce the effect significantly.

6 ACKNOWLEDGEMENTS

The authors thank the Canadian Space Agency and Environment Canada for providing data. This work was partly funded by MacDonald Dettwiler and Associates under contract to the Canadian Space Agency (No. 9F028-0-4902/06) as part of the Earth Observation Applications Development Program.

7 REFERENCES

1. Ferro-Famil L., Pottier E., and Lee J.S., Unsupervised Classification of Multifrequency and Fully Polarimetric SAR Images Based on the H/A/Alpha-Wishart Classifier, *IEEE Trans. Geosci. Remote Sensing*, vol. 39, no. 11, pp. 2332-2342, November 2001

2. Scheuchl B., Hajnsek I., Cumming I.G., Sea Ice Classification Using Multi-Frequency Polarimetric SAR Data, in *Proc. IGARSS'02*, Toronto, June 2002.

3. Lee J.S., Grunes M., Pottier E. and Ferro-Famil L., Segmentation of polarimetric SAR Images that Preserves Scattering, *Proceedings of EUSAR'2002*, Köln, 2002

4. Drinkwater M.R., Kwok R., Rignot E., Israelsson H., Onstott R.G. and Winebrenner D.P., Potential Applications of Polarimetry to the Classification of Sea Ice, in F. Carsey, *Microwave Remote Sensing of Sea Ice, AGU Geophysical Monograph 68*, 1992

5. Freeman T., and Durden S.L., A Three-Component Scattering Model for Polarimetric SAR Data, *IEEE Trans. Geosci. and Remote Sensing*, vol. 36, no. 3, pp. 963-973, May 1998

6. Scheuchl B., Hajnsek I., Cumming I.G., Model-Based Classification of Polarimetric SAR Sea Ice Data, in *Proc. IGARSS'02*, Toronto, June 2002.

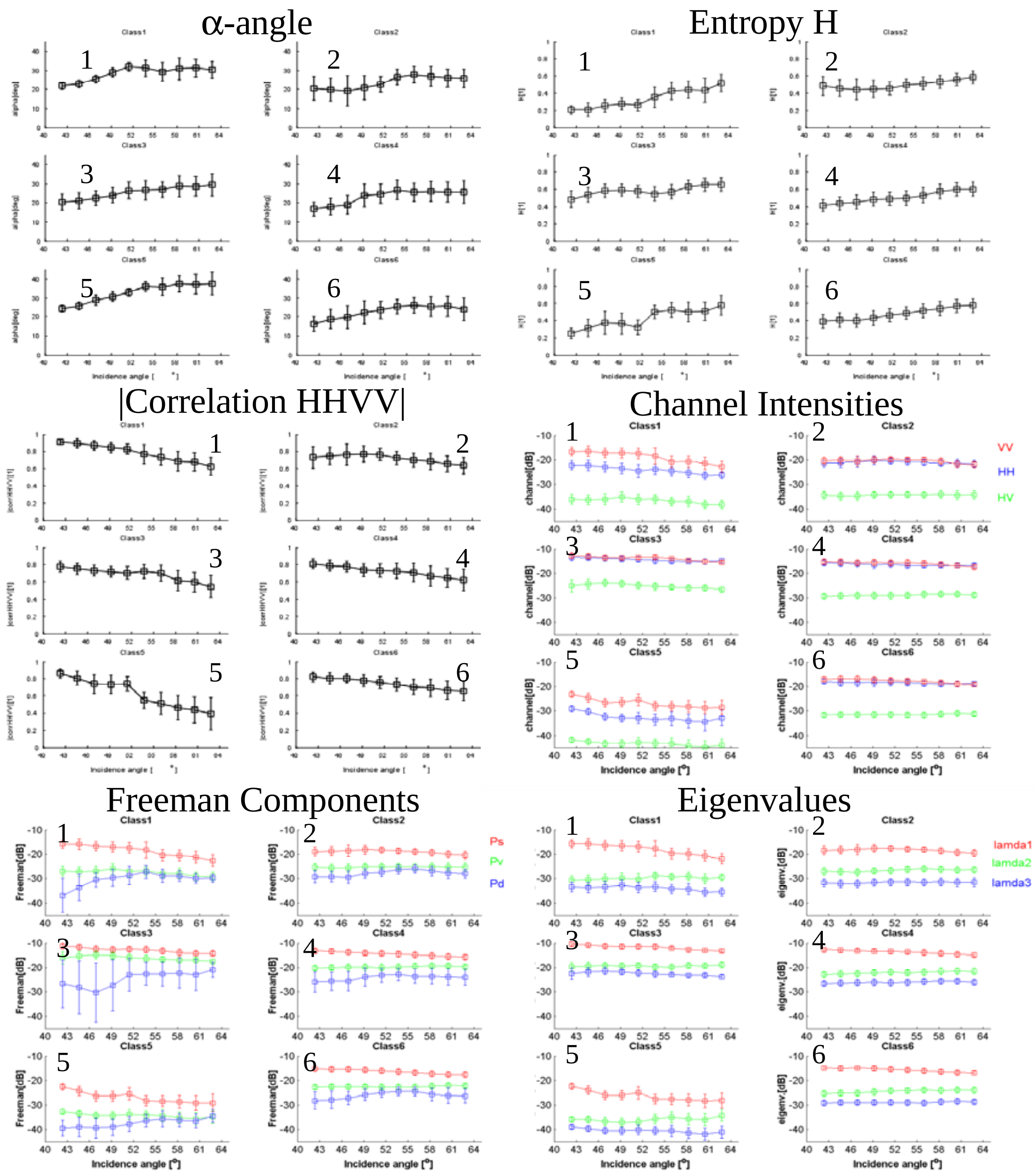

Fig. 5. Incidence angle dependence of polarimetric parameters. Test site: Northumberland Strait. One separate plot for each class (see Fig. 4 and Table 4) is provided.